Bioconjugate Chemistry

Article

pubs.acs.org/bc

Size-Stable Solid Lipid Nanoparticles Loaded with Gd-DOTA for Magnetic Resonance Imaging

Erica Andreozzi,[†] Peter Wang,[†] Anthony Valenzuela,[§] Chuqiao Tu,[†] Fredric Gorin,[§] Marc Dhenain,[‡,#] and Angelique Louie*[,†]

[†]Department of Biomedical Engineering, University of California Davis, Davis, California 95616, United States

[‡]CNRS, URA CEA CNRS 2210, 18 route du Panorama, 92265 Fontenay aux Roses, France

[#]CEA, DSV, I[2]BM, MIRCen, 18 Route du Panorama, 92265 Fontenay aux Roses, France

[§]Department of Neurology, School of Medicine, University of California Davis, 4860 Y Street, #3700, Sacramento, California 95817, United States

ABSTRACT: Solid lipid nanoparticles (SLNs) have recently emerged as nontoxic, versatile alternatives to traditional carriers (liposomes, polymeric nanoparticles) for drug delivery. Because SLNs are composed of a solid lipid core, they offer significant protection against chemical degradation of their drug cargo and offer the potential for controlled release. SLNs also hold promise for use as targeted agents and multimodal imaging agents. Here we report the synthesis and characterization of SLNs loaded with gadolinium (1,4,7,10-tetraazacyclododecane)-1,4,7,10-tetraacetate (Gd-DOTA) in order to produce a new category of stable T_1-weighted (T_1w) magnetic resonance imaging (MRI) contrast agents. Systematically varying components in the SLN synthesis, we demonstrated an increase in Gd-DOTA incorporation and an increase in longitudinal relaxivity (r_1) through optimizing the amount of surfactant (Span 80) in the "oil" phase. These highly monodisperse SLNs confirm stable loading of Gd-DOTA and a stable size distribution (~150 nm) over time in aqueous solution. Relaxivity measurements (1.4T, 37 °C) demonstrate that the r_1 of Gd-DOTA does not strongly decrease following encapsulation in SLNs, demonstrating an advantage over liposomes. These Gd-loaded SLNs demonstrate enhanced contrast *in vivo* at 7T using T_1w MRI and in the future can be loaded with other cargo (hydrophilic or hydrophobic) to enable functionality with other imaging modalities such as optical or positron emission tomography.

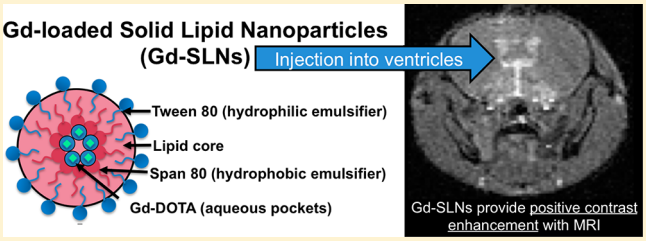

INTRODUCTION

Many lipid-based drug delivery systems (i.e., liposomes, lipoproteins, solid lipid nanoparticles, etc.) are currently under development to modify drug delivery properties and to protect bioactive cargo from degradation and/or deactivation.[1] Solid lipid nanoparticles (SLNs) are biocompatible submicrometer colloidal carriers consisting of a solid lipid core and a phospholipid monolayer that serve as versatile alternatives to these traditional carriers for drug delivery.[2−5] They are less toxic than polymer nanoparticles and have a better control over release than liposomes. Because SLNs are composed of a solid lipid core instead of the aqueous core characteristic of liposomes, they offer better protection against chemical degradation of their drug cargo.[2,6] As they biodegrade, SLNs facilitate sustained drug release due to the zero-order kinetic breakdown of the solid lipid matrix,[7,8] while liposomes tend to elicit a "burst" effect due to the nature of their aqueous core.[9] Thus, in comparison to liposomes, SLNs offer the advantages of better protection against chemical degradation potential for longer release profiles *in vivo*.[10]

SLNs have demonstrated controlled release under various administration routes[5,6,10−14] in the brain,[15,16] in tumors,[17−20] in ocular applications,[21−24] in lungs,[25−27] and in skin.[28−34] They have also been used as targeted agents by (1) modifying their charge[35−45] (i.e., cationic) or surfactant[14,46−51] (i.e., poloxamers, polysorbates, etc.), or (2) conjugating them with ligands[16,52,53] for cellular targets. In addition to their role as drug carriers, SLNs also have the potential to be used as multimodal imaging agents; we have previously encapsulated fluorophores inside SLNs and radiolabeled them for combined optical imaging and positron emission tomography.[54] Others have reported incorporation of Tc-99m[55] and quantum dots.[38,56−58]

While many studies have reported SLN encapsulation of therapeutic agents,[3,59−61] very few have reported encapsulation of diagnostic agents, especially for magnetic resonance imaging (MRI) applications.[15] One recent study described the ability to create SLNs with surface bound gadolinium (Gd) using lipid-bound gadolinium diethylenetriaminepenta acetic acid (Gd-DTPA) molecules.[62] The resulting Gd-lipid nanoparticles (Gd-LNP) produced a 33-fold higher longitudinal relaxivity (r_1) constant than free Gd-DTPA, likely due to restricted rotation of

Received: November 14, 2012
Revised: August 1, 2013

   dx.doi.org/10.1021/bc300605f | *Bioconjugate Chem.* XXXX, XXX, XXX−XXX

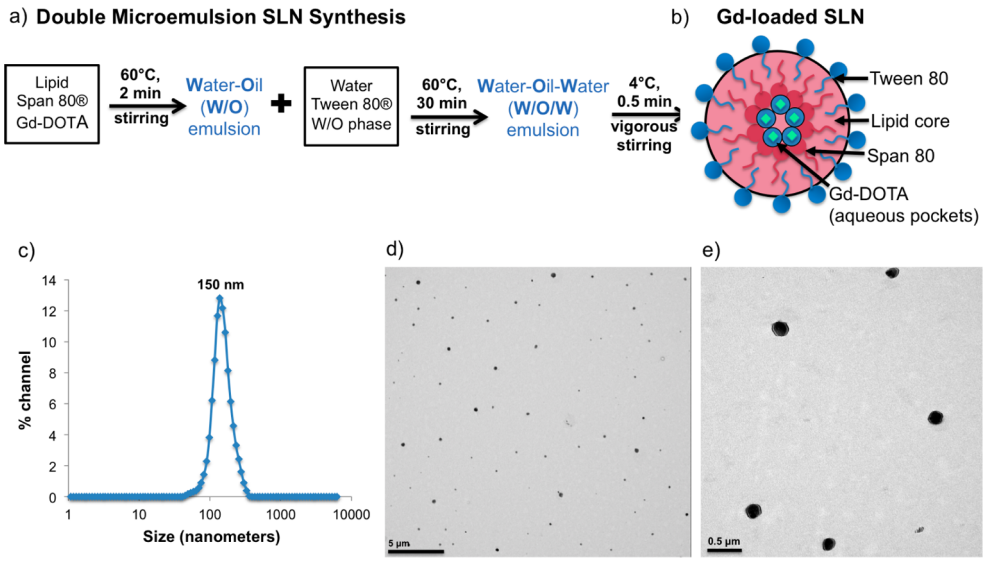

Figure 1. (a) Schematic of the double microemulsion synthesis used to form Gd-loaded SLNs (Gd-SLNs). (b) Schematic of a Gd-SLN suspended in water. Aqueous pockets of Gd-DOTA are dispersed inside the solid lipid core (glycerol monocaprate). Span 80 (dark pink) serves as the hydrophobic emulsifier and Tween 80 (blue) serves as the hydrophilic emulsifier. The SLN is stable in aqueous solution because of its phospholipid monolayer (blue) at the surface. (c) Dynamic light scattering (DLS) showing an average size of 151.0 ± 4.0 for the initial synthesis (Table 1a). Transmission electron microscopy (TEM) of the Gd-SLNs at low magnification (d) and high magnification (e) confirms a uniform, monodisperse particle distribution with a mean diameter of 149.3 ± 32.5 nm (n = 500).

the bound Gd-DTPA. These Gd-LNP demonstrated T_1-weighted (T_1w) contrast enhancement in the vasculature up to 24 h.[62] Very few other studies have explored encapsulating the paramagnetic payload inside of SLNs.[62−65] Peira et al. encapsulated T_2 contrast agents such as iron oxides (Endorem) into SLNs (SLN-Fe). They showed that SLN-Fe has similar relaxometric properties to Endorem *in vitro*.[63] Further evaluation of the SLN-Fe *in vivo* using MRI at 4.7T demonstrated that these lipid nanocarriers have slower blood clearance than Endorem following intravenous injection in rats, and that they are able to transport iron oxides across the blood brain barrier (unlike Endorem).[63] Aside from successful SLN encapsulation of T_2 MRI agents, there has also been one successful incorporation of Gd-DTPA into SLNs.[62] Following transrectal administration, these SLNs efficiently absorbed into the colorectal walls to provide positive MR contrast enhancement at 3T.[66]

Despite these first successes, further work is required to improve the Gd-loading of SLNs and to evaluate the performance of these contrast agents *in vivo*. The task of incorporating sufficient Gd chelates into SLNs is quite challenging because of the hydrophobic nature of the solid lipid core and the hydrophilic nature of the Gd chelate cargo. Hu et. al confirmed higher loading (~60%) of a hydrophilic peptide, gonadorelin, into SLNs (~450 nm)[67] using a solvent diffusion method. This solvent diffusion method was also used to load insulin (another hydrophilic peptide) into SLNs (~150 nm),[68] but our objective was to avoid the use of potentially toxic organic solvents. Another method used for the encapsulation of hydrophilic molecules into SLNs involves the formation of a hydrophobic ion pair between the hydrophilic molecule and an anionic salt. Cisplatin, a hydrophilic antitumor agent, was also loaded into SLN (275−525 nm) after formation of a hydrophobic ion pair between cisplatin and sodium dioctylsulfosuccinate.

Our approach was to use a double microemulsion synthesis involving a water−oil (W/O) primary emulsion and a water−oil−water (W/O/W) double emulsion (Figure 1). A double microemulsion is an emulsion system where small water droplets are entrapped within larger oil droplets that are in turn dispersed in a continuous water phase.[69] This microemulsion-based synthesis has been successful in the incorporation of water-soluble peptides,[4,6,70] proteins,[71−74] and other hydrophilic molecules[1,29,75−77] inside SLNs. The success of such incorporation has relied on relatively high solubility of the hydrophilic drug inside the primary emulsion. Adjustment of various parameters (i.e., type/amount of surfactant/oil) in the preparation of SLNs facilitates effective control of both encapsulation efficiency and release rate of encapsulated cargo.[69,72,73,75,78,79]

Herein, we report the synthesis and characterization of SLNs that demonstrate stable loading of Gd-DOTA and a stable size distribution (~150 nm) over time *in vitro*. Through measurements at 1.4T, we demonstrate that longitudinal relaxivity (r_1) of Gd-DOTA is not strongly decreased following encapsulation in SLNs. We also show that the amount of Gd-DOTA loaded inside the SLNs is large enough to provide contrast enhancement *in vivo* at micromolar Gd concentrations using T_1w MRI at 7T.

EXPERIMENTAL PROCEDURES

Materials. 1-Decanoyl-*rac*-glycerol (glycerol monocaprate), Span 80 (sorbitan monooleate), and sodium taurodeoxycholate hydrate (TDC, taurodeoxycholic acid sodium salt hydrate) were purchased from Sigma-Aldrich. Tween 80 (polyoxyethylene (20) sorbitan monooleate) and soybean lecithin was purchased from Fisher Scientific. Gd-DOTA ($GdC_{16}H_{24}N_4O_8Na{\cdot}4H_2O$, FW = 652.7 g/mol) was purchased from Macrocyclics. 14:0 PE-DTPA (Gd) 1,2-dimyristoyl-*sn*-glycero-3-phosphoethanolamine-*N*-diethylenetriaminepentaacetic acid (gadolinium salt) (i.e., lipid-Gd-DTPA) was purchased from Avanti Polar Lipids, Inc. Ultrafiltration membranes (MWCO = 30 000 Da) and centrifugal spin filters (Amicon Ultra) were purchased from Millipore. Spectra/Por dialysis

dx.doi.org/10.1021/bc300605f | *Bioconjugate Chem.* XXXX, XXX, XXX−XXX

Table 1. Systematic Variations to SLN synthesis for Increasing Gd-DOTA Incorporation[‡]

SLN synthesis parameters	load of Gd into SLN (w/w%)	Gd:SLN (mg/mg)	Gd:SLN (mol/mol)	r_1 ($mM^{-1}s^{-1}$)	size (nm)
(a) initial	7	0.07	0.03	2.67	**151.0 ± 4.0**
		variations to initial synthesis			
(b) initial, TDC	3	0.03	0.01	N/A	13.2 ± 3.7
(c) initial, 1/2 water in W/O	7	0.07	0.03	2.65	154.3 ± 6.5
(d) initial, 1/4 water in W/O	7	0.07	0.03	2.61	153.4 ± 5.1
(e) initial + lecithin	5	0.05	0.02	2.53	157.2 ± 7.6
(f) initial + lecithin + TDC	5	0.05	0.02	2.32	158.5 ± 5.4
(g) initial, 2× Span 80	**19**	**0.19**	**0.08**	**3.34**	**152.6 ± 5.0**
(h) initial, 3× Span 80		†	†	†	248.7 ± 9.2
(i) initial, 4× Span 80		†	†	†	282.3 ± 8.5
(j) initial + lipid-GdDTPA	21	0.21	0.09	20.66	99.5 ± 6.3

†We did not characterize these SLNs (h and i) further with inductively coupled plasma mass spectrometry (ICP-MS) and relaxivity because particles >200 nm would not be useful for our applications since they would trigger rapid clearance by the reticuloendothelial system.[83−85] ‡ Systematic variations (b-i) were made to the initial SLN synthesis (a) in an attempt to increase Gd-DOTA encapsulation. One variation (b) decreased SLN size. Two variations (g and j) increased the Gd:SLN ratio as well as longitudinal relaxivity (r_1) at 1.4T (37°C). The average hydrodynamic diameter for all SLN syntheses (except b, h, and i) was ∼150 nm.

membranes (MWCO = 2000 Da) were purchased from Spectrum Laboratories. Formvar Coated Copper Grids (300 Mesh) were purchased from SPI Supplies (West Chester, PA). Normal mice (C57BL6) were purchased from Harlan.

Synthesis and Purification of SLNs Loaded with Gd-DOTA. *Initial Synthesis.* Gd-DOTA was loaded into SLNs using a modified warm water−oil−water (W/O/W) double microemulsion method.[71] First, a mixture of glycerol monocaprate (10 mg, 0.04 mmol), Span 80 (7.1 μL, 14.0 mg, 0.03 mmol), and Gd-DOTA (11 mg, 0.02 mmol dissolved in 150 μL nanopure water) were warmed at 60 °C, forming a W/O ("oil" phase) emulsion. This W/O ("oil" phase) emulsion was then introduced into a warm (60 °C) W/O/W ("aqueous" phase) emulsion consisting of water and Tween 80 (1 μL, 1.08 mg, 0.8 μmol). This resulting mixture was heated (60 °C) for 30 min and then pipetted into vigorously stirring ice water (4 °C), forming an SLN suspension. Free, unencapsulated Gd-DOTA was removed from the SLN suspension via ultrafiltration (30 000 MWCO membrane, Amicon Millipore ultrafiltration cell) and dialysis (10 000 MWCO) purification methods. The final SLN dose was concentrated using centrifuge membrane-filters (3000 MWCO).

Modifications for Smaller Size and Higher Gd-DOTA Encapsulation. Modifications to the initial SLN synthesis method (described above) were made in order to decrease particle size diameter and to increase the loading of Gd-DOTA inside the particle. First, in an attempt to decrease the particle size diameter of the Gd-SLNs, sodium taurodeoxycholate hydrate (5 mg, 0.01 mmol) was added to the secondary W/O/W ("aqueous" phase) emulsion, consisting of water and Tween 80. Next, in an attempt to increase the loading of Gd-DOTA inside the particle, several systematic variations (Table 1c-j) were made to the initial synthesis. For variations c and d, the amount of water in the W/O ("oil" phase) emulsion was decreased to 1/2 and 1/4 of the original amount, respectively, resulting in a 2-fold and 4-fold increase of Gd-DOTA concentration. For variation e, soybean lecithin (5 mg, 0.007 mmol) was added as an additional ingredient to the W/O ("oil" phase) emulsion. The same was true for variation f, except with the addition of TDC (5 mg, 0.01 mmol) alongside the addition of lecithin. For variation g, the amount of Span 80 in the W/O ("oil" phase) emulsion was doubled from 7.1 μL (14.0 mg, 0.03 mmol) to 14.2 μL (28.0 mg, 0.06 mmol). We also tripled (h) and quadrupled (i) the amount of Span 80 in the W/O ("oil" phase) emulsion after observing the increase of Gd-DOTA incorporation that resulted from doubling Span 80. For variation j, 5 mg (0.004 mmol) of the lipid-Gd-DTPA molecule, 14:0 PE-DTPA (Gd) 1,2-dimyristoyl-*sn*-glycero-3-phosphoethanolamine-*N*-diethylenetriaminepentaacetic acid (gadolinium salt), was added as an additional ingredient to the primary W/O ("oil" phase) emulsion. The temperature/heating time conditions and the purification methods were the same for the modified SLN syntheses (Table 1b-j) as they were for the initial synthesis (Table 1a).

Determination of Gd-SLN Size and Monitoring of Size Stability over Time. The mean hydrodynamic diameter (intensity-weighted) of the purified Gd-SLN suspension was determined using dynamic light scattering (DLS) immediately following synthesis (Nanotrac 150 particle size analyzer, Microtrac), and monitored every day (up to 2 weeks) in aqueous solution. The mean hydrodynamic diameter and polydispersity index (PDI) were calculated by the Microtrac software, which uses frequency spectrum analysis to convert detected frequency values to particles size from Brownian motion theory. Particle size was also measured using transmission electron microscopy (TEM) (CM120 Biotwin Lens, FEI Company, Hillsboro, OR, U.S.A.) operating at 80 keV. The Gd-SLN suspension was diluted 20-fold and plated onto Formvar coated copper grids (300 Mesh) to dry overnight. Images were analyzed using *ImageJ* software (National Institutes of Health) and n = 500 particles were measured to yield average particle diameter.

Determination of Gd Content inside Gd-SLNs and Loss of Gd Content over Time. Inductively coupled plasma mass spectrometry (ICP-MS) was used to measure the Gd content of the Gd-SLN suspension. The prepared samples were analyzed using an Agilent 7500CE ICP-MS (Agilent Technologies, Palo Alto, CA). The samples were introduced using a MicroMist Nebulizer (Glass Expansion 4 Barlow's Landing Rd., Unit 2A Pocasset, MA 02559) into a temperature controlled spray chamber. The Gd instrument standards were diluted from Certiprep ME 1 (SPEX CertiPrep, 203 Norcross Avenue, Metuchen, NJ 08840) to 0.25 ppb, 0.5 ppb, 1 ppb, 10 ppb, 100 ppb, and 500 ppb respectively in 3% Trace Element HNO_3 (Fisher Scientific) in 18.2 milliohm water. A separate 10 ppb Certiprep ME 1 Standard was analyzed every 10th sample as a

dx.doi.org/10.1021/bc300605f | *Bioconjugate Chem.* XXXX, XXX, XXX−XXX

quality control. Sc, Y, and Bi Certiprep standards (SPEX CertiPrep) were diluted to 100 ppb in 3% HNO_3 and introduced by a high precision peristaltic pump (peripump, Omaha, NE 68110) as an internal standard. The detection limit of Gd using this ICP-MS method is 0.004 ppb (0.004 ng/mL).

Lyophilization of the same Gd-SLN suspension analyzed by ICP-MS enabled us to determine the dry weight of the Gd-SLNs, from which we could approximate the Gd:SLN (mg/mg, mol/mol) ratio from the molecular weight of the lipid and Gd-DOTA components. Furthermore, this Gd-SLN suspension was placed on dialysis (MWCO = 1000) for three weeks, and the Gd content in the reservoir outside the dialysis membranes was measured with ICP-MS. Any increase of the Gd content in the reservoir over time would indicate that the Gd-SLNs were breaking down and releasing their Gd-DOTA cargo.

Cytotoxicity Assay of the Gd-SLNs. Cytotoxicity of the Gd-SLNs was evaluated with P388D1 (murine macrophage) cells using the C_{12}−Resazurin viability assays.[80] The P388D1 cells were maintained in tissue culture flasks (75 cm^2) in media (RPMI-1640 with 1% L-glutamine and 10% fetal bovine serum (FBS)) and incubated at 37 °C and 5% CO_2 atmosphere. When the cells reached 80−90% confluency, the media was removed. The cells were scraped down with a rubber policeman and were plated in 96-well dishes at a concentration of 1.2×10^4 cells per well, an optimal seeding density for this cytotoxicity assay. After overnight incubation (5% CO_2, 37 °C), the existing RPMI-1640 was replaced with fresh media containing varying concentrations of Gd-SLNs (variation g, Table 1). Cells were incubated with the Gd-SLNs for either 4 or 24 h and then the media was removed. After that, the cells were washed with 1× PBS three times and media containing C_{12}−Resazurin (5 μM) was added. Following 15 min incubation for reduction of the compound, fluorescence was measured using a Safire2 monochromator microplate reader (Tecan Austria G.M.B.H., Austria) with excitation of 563 nm and emission of 587 nm. Samples were performed in triplicate to provide statistical significance and the experiment was repeated to confirm the results.

Relaxivity of Gd-SLNs at 1.4 T. Longitudinal relaxivity (r_1) of the Gd-SLNs were measured at 60 MHz (1.4T) and 37 °C on a Bruker Minispec mq60 (Bruker, Billerica, MA). A stock solution of Gd-SLNs was prepared (in triplicate) by dissolving known amounts of lipid (by weight) in deionized water (pH 7.0). The concentration of Gd in this stock solution was determined by ICP-MS. Serial dilutions of these stock solutions yielded five different aqueous solutions (0.3 mL each) with decreasing Gd concentration. T_1 values were measured using an inversion recovery sequence with 10−15 data points, with each solution having been incubated at 37 °C for 10 min before measurement. The longitudinal relaxivity (r_1) was determined as the slope of the line for plots of $1/T_1$ against Gd concentration with a correlation coefficient greater than 0.99.

MR Imaging of Gd-SLN Solutions at 7 T. MR images were acquired for solutions of the Gd-SLN by two different T_1w protocols. Images of Gd-SLN solutions (variation g, Table 1, ∼150 nm) at different concentrations of Gd (0.3, 0.6, 1.1, 2.2, and 4.5 mM) were acquired to demonstrate T_1w signal enhancement with an increase in Gd concentration (2D spin echo sequence, repetition time (TR) = 421.1 ms, echo time (TE) = 12.0 ms, in plane spatial resolution = 188 × 375 μm^2, slice thickness = 1.0 mm, 7T Bruker spectrometer equipped with a 72 mm diameter bird cage probe).

We then recorded images of vials containing nanopure water, Gd-SLNs, and Gd-DOTA diluted in saline at the same Gd stock concentration (1.525 mg Gd/ml, 9.7 mM) used for the *in vivo* studies (2D gradient echo sequence, TR/TE/flip angle (α) = 500 ms/5.31 ms/30°, in plane spatial resolution = 243 × 239 μm^2, slice thickness = 1.3 mm). All samples were maintained at room temperature (25 °C) during imaging.

T_1w MRI at 7T following ICV Injection of Gd-SLNs into Mice. *ICV Technique.* ICV injection of the Gd-SLNs was completed according to a protocol approved by the UC Davis Institutional Animal Care and Use Committee. First, mice (n = 6) were anesthetized with isofluorane (2.5%, inhalation route) and placed into a stereotaxic device maintained at 37 ± 0.2 °C on a feedback-controlled heating pad. The scalp was shaved and prepared with 3 cycles of betadine scrub and 70% isopropyl alcohol before the incision. A small burr hole was drilled into the skull of the mice at −0.2 mm anterior and 1.0 mm lateral (−1.0 for left ventricle, 1.0 for right ventricle) to bregma.[81] A Hamilton syringe with 26 gauge needle was lowered 1.8 mm into the brain and 2 μL of contrast agent (Gd-SLNs or free Gd-DOTA) was injected at a rate of 2 μL/minute. The Gd concentration of the delivered contrast agent was 9.7 mM; this yields a dose of 7.8×10^{-4} mM/kg per mouse. The needle was maintained inside the ventricle for 2 min before being withdrawn. For each mouse, the left ventricle was injected first, followed by the right ventricle, with 10 min of preparation time in between. Free Gd-DOTA in saline (0.9%) was injected into the left and right ventricles of mice (n = 3) to serve as a control for comparison against the mice (n = 3) injected with Gd-SLNs. Following removal of the syringe from the ventricle, the incision was sutured and Buprenex (0.1 mg/kg) was delivered subcutaneously as a post-op analgesic.

T_1w MRI. The mice were anesthetized with isoflurane (5% for induction and 1−2% for maintenance) during the scans. T_1w MRI (3D gradient echo images, TR/TE/α = 25 ms/2.75 ms/30°, spatial resolution = 188 × 188 × 188 μm^3, 7T Bruker equipped with a 25 mm diameter bird cage probe) was used to observe the contrast enhancement generated 55, 75, 85, and 100 min after ICV injection of Gd-SLNs. Animals were kept in the MRI between the scans.

Quantifying Changes in Signal Intensity in T_1w Images over Time. Region of interest (ROI) analysis was performed on the T_1w images in order to characterize the changes in signal intensity within the ventricles and other brain regions over time. The T_1w images were viewed with *ImageJ* software (NIH), and circular ROIs were drawn bilaterally in the following regions: ventricle, striatum, parietal cortex, septum, muscle (outside the brain), and background (outside the tissue region) (Figure 3d). The ROI area was equal to 0.6 mm^2 for all regions except the background, which had a larger area (∼120 mm^2). The representative slice from the T_1w MRI data sets that was chosen for ROI analysis was the slice that depicted the interventricular foramen (where the lateral ventricles meet the third ventricle). Contrast-to-noise ratio (CNR) was calculated for the various brain regions (following ICV injection of both Gd-SLNs and free Gd-DOTA) using the following equation

$$\mathrm{CNR} = \frac{\text{mean signal intensity in brain ROI} - \text{mean signal intensity in muscle}}{\text{standard deviation of background}}$$

Statistical Analysis. Statistical analyses of CNR changes in the T_1w images in the ventricles, septum, parietal cortex, and striatum were analyzed using a repeated measure ANOVA with

dx.doi.org/10.1021/bc300605f | Bioconjugate Chem. XXXX, XXX, XXX−XXX

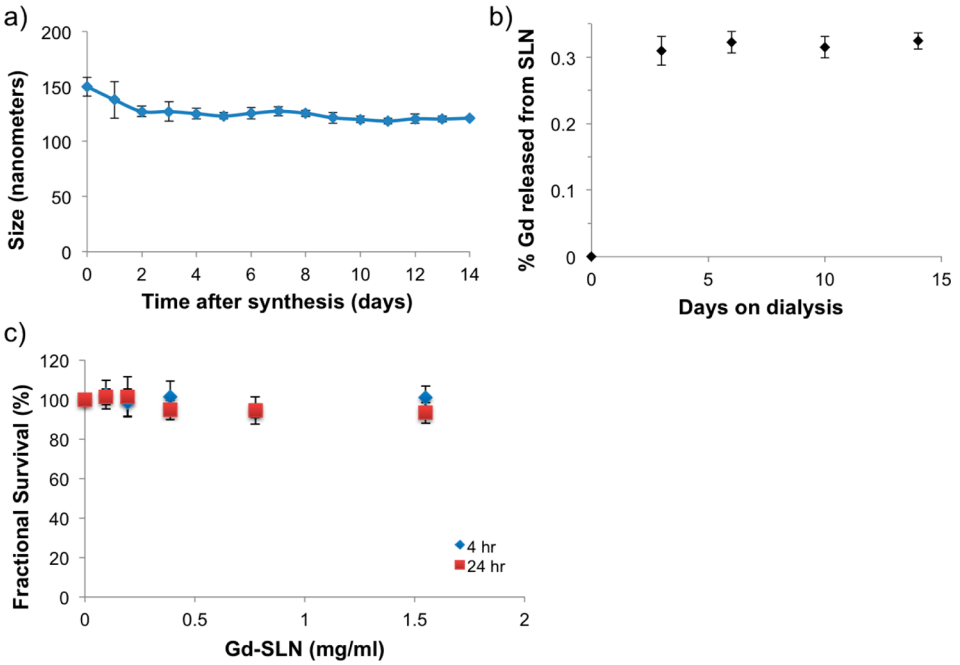

Figure 2. (a) DLS verifies that the size of the Gd-SLNs (variation g, Table 1, ~150 nm) was stable up to 14 days in aqueous solution. (b) ICP-MS confirms that the Gd content in the Gd-SLN (variation g, Table 1, ~150 nm) dialysis reservoir is not increasing over time. (c) Cell viability of P388D1 after 4 h (blue diamonds), or 24 h (red squares) incubation with different concentrations of Gd-SLNs (variation g, Table 1, ~150 nm).

time and contrast agent as variables. Posthoc analyses were performed to analyze time effect for each contrast agent. Statistica 7.1 (StatSoft, Inc., Tulsa, USA) was used for all the analysis. Two-tailed $p < 0.05$ was considered statistically significant.

RESULTS AND DISCUSSION

Synthesis of Gd-Loaded SLNs (Gd-SLNs) using W/O/W Double Microemulsion. We developed a synthetic strategy for loading Gd-DOTA into SLNs, and later systematically varied the components (i.e., lipid, emulsifier, and water) in order to maximize loading of Gd-DOTA into the SLNs while maintaining appropriate size (<200 nm). We also modified the synthesis to control particle size and investigated the different loading properties of larger and smaller particles. Our initial synthesis was based on a modified warm W/O/W double microemulsion described by Li et al. for the encapsulation of bovine serum albumin (BSA).[71] The warm W/O/W double microemulsion method is a relatively simple and efficient way to prepare SLNs loaded with unstable and hydrophilic drugs and proteins. In this method, the W/O/W double microemulsion (lipid micelles in aqueous solution) contains smaller dispersed droplets of the primary (W/O) emulsion (lipid micelles containing aqueous pockets of hydrophilic cargo).[82] A schematic of this double microemulsion synthesis and the Gd-loaded SLNs that result from this synthesis is shown in Figure 1a,b.

W/O/W double emulsions require at least two emulsifiers to be present in the system, one that has a low hydrophilic–lipophilic balance (HLB) value to stabilize the primary W/O emulsion, and one that has a high HLB value to stabilize the secondary W/O/W emulsion.[69] The low HLB surfactant is dominantly hydrophobic and is added to the primary W/O ("oil" phase) emulsion to facilitate solubility of the hydrophilic drug in oil. In the second step, the primary W/O ("oil" phase) emulsion is re-emulsified by aqueous solution with a high HLB surfactant to produce a double W/O/W ("aqueous" phase) emulsion.[71] A high concentration ratio of these two surfactants is required for obtaining a high yield of stable double W/O/W microemulsion systems such as SLNs, in which small water droplets are entrapped within larger oil droplets that in turn are dispersed in water.[69] In our work, the primary W/O ("oil" phase) emulsion is prepared from a warm mixture of lipid (glycerol monocaprate), low HLB emulsifier (Span 80, HLB = 4.3), and hydrophilic cargo (Gd-DOTA dissolved in water). The primary W/O ("oil" phase) emulsion is then dispersed in the secondary W/O/W ("aqueous" phase) emulsion, containing Tween 80 and water (Figure 1a). Finally, this double emulsion is dispersed into vigorously stirring ice water (4 °C), forming SLNs that contain a hydrophobic emulsifier (Span 80, HLB = 4.3) at the surface of the SLN's lipid core and a hydrophilic emulsifier (Tween 80, HLB = 15) at the surface of the SLN monolayer (Figure 1b).

The outcome of the SLN synthesis was analyzed with dynamic light scattering (DLS), transmission electron microscopy (TEM), relaxometry, and inductively coupled plasma mass spectrometry (ICP-MS). DLS was used for determination of hydrodynamic diameter and confirmed a unimodal, Gaussian size distribution for the SLNs with an average value of 151.0 ± 4.0 nm (Figure 2c) and a polydispersity index of 0.25. From the TEM images in Figure 1d and e, we observe that the SLNs exist as a uniform, highly monodisperse population of spherical particles with a diameter of 149.3 ± 32.5 nm (n = 500 particles). The larger standard deviation by TEM may be due to effects of drying and sample preparation. By either measurement, the SLNs fall into the 20–200 nm size range reported for particles capable of avoiding rapid clearance through the kidneys,[2,83−85] thus making them attractive carriers for *in vivo* contrast agent or drug delivery.

Longitudinal relaxivity (r_1) measured at 1.4 T (37 °C) yielded a value of 2.67 mM^{-1} s^{-1} for the initial synthesis (Table 1a). ICP-MS was used to determine the Gd content of the Gd-

dx.doi.org/10.1021/bc300605f | *Bioconjugate Chem.* XXXX, XXX, XXX−XXX

SLN suspension; lyophilization of this same suspension enabled us to determine the dry weight of the Gd-SLNs, from which we could approximate the Gd:SLN (mg/mg, mol/mol) ratio from the molecular weight of the lipid and Gd-DOTA components. The initial synthesis (Table1a) produced Gd-SLNs with a Gd:SLN ratio of 0.07 mg/mg (~0.03 mol/mol). The Gd:SLN ratio (Table 1, mg/mg or mol/mol) was the main criteria used for identifying the effectiveness of Gd-DOTA incorporation into the SLN matrix.

Modifications to Synthesis for Enhanced Loading of Gd-DOTA inside the SLNs. The initial synthesis (Table 1a) was then modified with systematic variations of the primary W/O ("oil" phase) emulsion and secondary W/O/W ("aqueous" phase) emulsion compositions (Table 1b-j). The outcomes of these synthetic variations (i.e., concentration of hydrophilic cargo, surfactant amount and type, and addition of extra emulsifier) were analyzed with DLS, relaxometry, and ICP-MS.

In an effort to decrease particle size, we added sodium taurodeoxycholate hydrate (TDC) to the secondary W/O/W ("aqueous" phase) emulsion (Table 1b). TDC is a bile salt and anionic detergent that is typically used to disrupt the phospholipid bilayer of a cell membrane for protein extraction[86,87] and also used for fat solubilization.[88] It has been investigated as a detergent for decreasing the size of micelles during various syntheses.[89] Previous studies show that the addition of bile salts (low mole fractions) like TDC decreases the size of micelles formed from nonionic surfactants (i.e., Tween 80).[90] This was observed for other studies in which micelles as small as 50 nm were synthesized only after addition of bile salts with other surfactants.[91] In another study the use of bile salts as cosurfactants was required to obtain particles with average diameters as small as 30 nm.[92,93] This was also the case for a related study in which small (~20 nm in diameter) micelles were found to form only after incorporation of bile salt into a surfactant mixture containing phosphatidylcholine.[94]

We found that the addition of TDC to the secondary W/O/W ("aqueous" phase) emulsion of the initial SLN synthesis (Table 1b) was effective in decreasing particle size (Table 1b). The average hydrodynamic diameter of these modified SLNs was 13.2 ± 3.7 nm, an order of magnitude lower than the average hydrodynamic diameter (151.0 ± 4.0 nm) for the initial synthesis (Table 1a). Although this variation of TDC addition was successful in decreasing particle size, it did so at the expense of decreasing Gd-DOTA incorporation, as seen by the decrease in ratio of Gd:SLN from ~0.03 mol/mol (initial synthesis, Table 1a) to ~0.01 mol/mol (TDC modified synthesis, Table 1b). Since the most important aim of the synthesis was to achieve maximal Gd-DOTA loading, we focused toward SLN modifications that increased Gd-DOTA incorporation rather than decreased particle size.

To increase Gd-DOTA loading, we modified the initial synthesis to increase the concentration of hydrophilic cargo Gd-DOTA inside the primary W/O ("oil" phase) emulsion of the initial SLN synthesis (Table 1c and d). Increasing Gd-DOTA concentration inside the W/O ("oil" phase) emulsion by decreasing the amount of water (1/2 and 1/4 for Table 1c and d) and keeping Gd-DOTA weight constant did not result in any increase in the Gd:SLN ratio (average size = 154.3 ± 6.5 nm and 153.4 ± 5.1 nm for both variations, Table 1c, d). Relaxivity measurements (1.4T, 37 °C) indicated r_1 values of 2.65 mM^{-1} s^{-1} and 2.61 mM^{-1} s^{-1} for variations c and d, respectively.

Also, addition of another emulsifier, lecithin, to the primary W/O ("oil" phase) emulsion of the SLN synthesis (Table 1e) or addition of two emulsifiers, lecithin and TDC, to the initial synthesis (Table 1f) did not have any effect on the Gd loading capacity of the SLNs. Relaxivity measurements (1.4T, 37 °C) indicated r_1 values of 2.53 mM^{-1} s^{-1} and 2.32 mM^{-1} s^{-1} for variations e and f, respectively. DLS measurements indicated average sizes of 157.2 ± 7.6 nm and 158.5 ± 5.4 nm for variations e and f, respectively (Table 1). This result differs from a previous study by You et al. where the addition of lecithin improved the loading capacity of the hydrophilic drug vinorelbine bitartrate.[95] This may be due to the differences in lipid and cargo type between studies; the main lipid component used in the You et al. study was oleic acid while it was glycerol monocarpate in our study.

In previous studies, surfactants had a distinct influence on the particle matrix structure, and its corresponding stability and drug loading capacity.[96] We therefore made systematic variations to the surfactant content to evaluate its effect on cargo encapsulation and particle size. Considering the hydrophilic nature of Gd-DOTA, we modified the reported synthesis to increase the amount of low (4−6) hydrophile−lipophile balance (HLB) emulsifier (Span 80, HLB = 4.3) in our warm W/O/W double emulsion synthesis in order to increase the loading efficiency of Gd-DOTA.

Doubling (2×) the amount of HLB emulsifier (compared to the initial synthesis) more than doubled the Gd:SLN ratio from 0.03 mol/mol (Table 1a) to 0.08 mol/mol (Table 1g). Particle size was not affected by this synthetic variation and DLS measurements indicated an average size of 152.6 ± 5.0 nm, very similar to the initial synthesis. Relaxivity determinations (1.4T, 37 °C) indicate that the increase in Gd encapsulation associated with variation g resulted in a 25% increase in r_1, moving from a value of 2.67 mM^{-1} s^{-1} (initial synthesis, Table 1a) to ~3.34 mM^{-1} s^{-1} (Table 1g). This confirms that increasing the loading of Gd-DOTA into SLNs can enhance the longitudinal relaxivity (r_1). The r_1 value for these Gd-SLNs (~3.34 mM^{-1} s^{-1} at 1.4T, variation g) was comparable to the r_1 values of free Gd-DOTA (~3.94 mM^{-1} s^{-1}).[97] The high r_1 relaxation reported for Gd-SLN is different than results reported for other lipid-based drug delivery systems such as liposomes. Indeed, encapsulation of Gd(III) complexes inside liposomes were shown to reduce r_1 by a factor of 2−5 times.[98] This could be attributed to the reduced exchange of water with Gd(III) complexes encapsulated inside the liposomes.[99] The high r_1 relaxation reported for Gd-SLN might be explained by the presence of aqueous pockets within the SLN and by the relaxation of this interior water. Interior water pockets could be associated with the hydrophilic portion of the amphipathic lipid (glycerol monocaprate) comprising the SLN matrix.

This technique of increasing HLB emulsifier content has previously been successful in enhancing SLN incorporation of hydrophilic components.[100] Other studies have shown that the HLB emulsifier we used (Span 80) has a stabilizing effect on double emulsion globules and that this oil-soluble surfactant is required for coalescence of such suspensions.[101] Nevertheless, there exists a threshold for which increased addition of Span 80 can actually affect particle size at the expense of the increased cargo encapsulation; increasing the Span 80 content beyond double (2×) the initial synthesis resulted in an increase of particle size. For example, tripling (3×) and quadrupling (4×) the amount of Span 80 in the W/O ("oil" phase) emulsion of the initial synthesis (double the amount of Span 80 in variation

g) increased the average hydrodynamic diameter to 248.7 ± 9.2 nm (Table 1h) and 282.3 ± 8.5 nm (Table 1i), respectively. We did not characterize these SLNs because particles larger than 200 nm would not be as useful for *in vivo* applications as they would trigger rapid clearance by the reticuloendothelial system.[83−85]

We also investigated tethering contrast agents to the surface of SLN. The commercially available lipid-Gd-DTPA molecule, 14:0 PE-DTPA (Gd) 1,2-dimyristoyl-*sn*-glycero-3-phosphoethanolamine-*N*-diethylenetriaminepentaacetic acid (gadolinium salt) was used in the initial synthesis (Table 1j). This adds a Gd-DTPA tethered to a lipid component of the SLN. DLS measurements indicated an average size of 99.5 ± 6.3 nm, which is smaller than the 151.0 ± 4.0 nm size from the initial synthesis. This variation resulted in similar gadolinium content to variation g, 0.09 mol/mol (Table 1j) vs 0.08 mol/mol (Table 1g), confirming that Gd-DTPA conjugated to lipid could be loaded to SLNs. However, SLN with surface tethered Gd-DTPA had a much larger longitudinal relaxivity (r_1= 20.66 mM^{-1} s^{-1}) than variation g (r_1= 3.34 mM^{-1} s^{-1}). This is likely because the lipid-Gd-DPTA incorporated at the surface of the SLN such that the Gd-DPTA was accessible to the aqueous environment; in addition, tethering likely resulted in slowed rotational tumbling time for the tethered Gd-DTPA, which is known to increase relaxivity.[102,103] These observations are similar to a study where a lipid-Gd-DTPA molecule was incorporated on the surface of liposomes for use in T_1w imaging applications.[62] These Gd-DTPA-liposomes were reported to have an r_1 value of 13.6 mM^{-1} s^{-1}at 3T (37 °C) compared to free Gd-DTPA which has r_1 of 3.8 mM^{-1} s^{-1} at 3T (25 °C).[62] Several other studies have confirmed the addition of Gd to the surface of a liposome using Gd conjugated to a lipid.[62,64]

Surface conjugation, however, does not protect the cargo (Gd-DOTA) from degradation or enable controlled release as a SLN would. Thus, we proceeded to carry out stability, cytoxicity, and imaging studies using variation g since this variation yielded the highest Gd-DOTA encapsulation. This variation displays the highest Gd:SLN ratio and the highest r_1 with Gd fully incorporated inside (not outside) the SLN.

Stability of SLN Size and Gd-DOTA Cargo over Time. Following purification through ultrafiltration methods, the SLNs were incubated in water at room temperature and sized every 24 h for up to 14 days. Figure 2a shows that the initial particle size (151.0 ± 4.0 nm) was stable over time in aqueous solution, confirming particle stability up to 14 days of evaluation.

Dialysis studies were performed to evaluate the stability of the Gd-DOTA cargo inside the Gd-SLNs (variation g). Gd-SLNs were placed inside the dialysis membranes and ICP-MS was used to monitor the release of Gd to the surrounding solution over time. Only a negligible amount of Gd (~0.3%) of the dialysate (Gd-SLNs inside the dialysis bags) was present in the dialysis reservoir 3 days after the start of dialysis (Figure 2b). This negligible amount of Gd did not increase over time up to 15 days (Figure 2b). This means that the SLN matrix was not breaking down and releasing Gd in aqueous solution up to 15 days. The stability studies were performed *in vitro* without lipases. Because SLNs are composed of physiological lipids, the stability *in vivo* will depend on exposure to physiologically relevant enzymes, particularly lipases, which split the ester linkage into glycerol and free fatty acids. Under the lipase-free conditions of our *in vitro* study, there is no further release of Gd-DOTA after the initial burst release (Figure 2b). One method to control release rates/degradation of SLN is to modify the amount of Tween 80 at the particle surface. Tween 80 is a steric stabilizer that is known to hinder SLN degradation by lipases.[104] This will be the topic of future studies.

Evaluation of of Gd-SLNs Cytotoxicity. In order to assess the toxicity of Gd-SLNs to cells, Gd-SLNs were applied to P388D1 (murine macrophage) cells in culture and the cell viability was evaluated by the C_{12}−Resazurin viability assay.[80] Untreated cells served as negative control. The average cell viability was above 94% or 93% after 4 or 24 h incubation with the particles varying from 0.10 mg/mL to 1.55 mg/mL solid lipid weight, respectively (Figure 2c). These results showed that the Gd-SLNs (variation g, Table 1) at concentrations relevant for biological imaging did not have observable toxicity to mammalian cells. Our results agree with the majority of the literature reporting low cytotoxicity of SLNs.[105−108] Also, as our SLNs were not tagged with fluorophores, we could not visualize whether they were actually taken up by the macrophages. However, several other studies on SLNs revealed an uptake of SLNs by macrophages and a low toxicity despite this uptake.[106,107,109,110]

As mentioned in the introduction, literature suggests that SLNs are less toxic than polymeric nanoparticles,[111−116] and Mehnert et al. summarizes these studies in a comprehensive review;[117] he discusses how different aspects of SLN composition and administration affect their safety and fate *in vivo*. One study reported much lower (2.5%) cell viability of human granulocytes after incubation with polymeric nanoparticles in comparison with SLNs (72%). Polylactide/polyglycolide (PLGA) nanoparticles were also shown to reduce cell viability to 50% at a concentration as low as 0.1% when similar concentrations of SLN proved less toxic.[116] Furthermore, many studies have demonstrated low SLN cytotoxicity toward a variety of cell types (granulocytes, macrophages, fibroblasts, lung endothelial cells, etc.).[116,118−121] For example, SLNs were shown to have neither direct nor indirect cytotoxic effects[106] on murine macrophages *in vitro*. These studies support our use of SLNs for safe delivery of contrast agents *in vivo*.

MRI of Gd-Loaded SLNs in Solution at 7T. We evaluated the ability of Gd-loaded solid lipid nanoparticles (Gd-SLNs) to provide positive contrast enhancement on T_1w MR images at 7T by either spin echo or gradient echo (Figure 3). T_1w MR spin echo images of Gd-SLNs (variation g, Table 1, ~150 nm) containing increasing concentrations of Gd (0.3, 0.6, 1.1, 2.2,

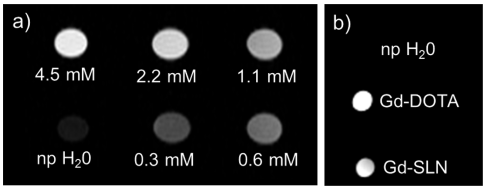

Figure 3. (a) T_1w MR images of Gd-SLNs solutions (variation g, Table 1, ~150 nm) containing various concentrations of Gd (0, 0.3, 0.6, 1.1, 2.2, and 4.5 mM) show an increased signal with increased Gd concentration. (b) T_1w MR images of Gd-SLNs (variation g, Table 1, ~150 nm) and free Gd-DOTA solutions containing the same Gd concentration as used for the *in vivo* experiments (1.525 mg Gd/ml, 9.7 mM) revealed an increased signal of Gd-SLN and Gd-DOTA solutions compared to nanopure water (negative control, invisible on this image).

dx.doi.org/10.1021/bc300605f | *Bioconjugate Chem.* XXXX, XXX, XXX−XXX

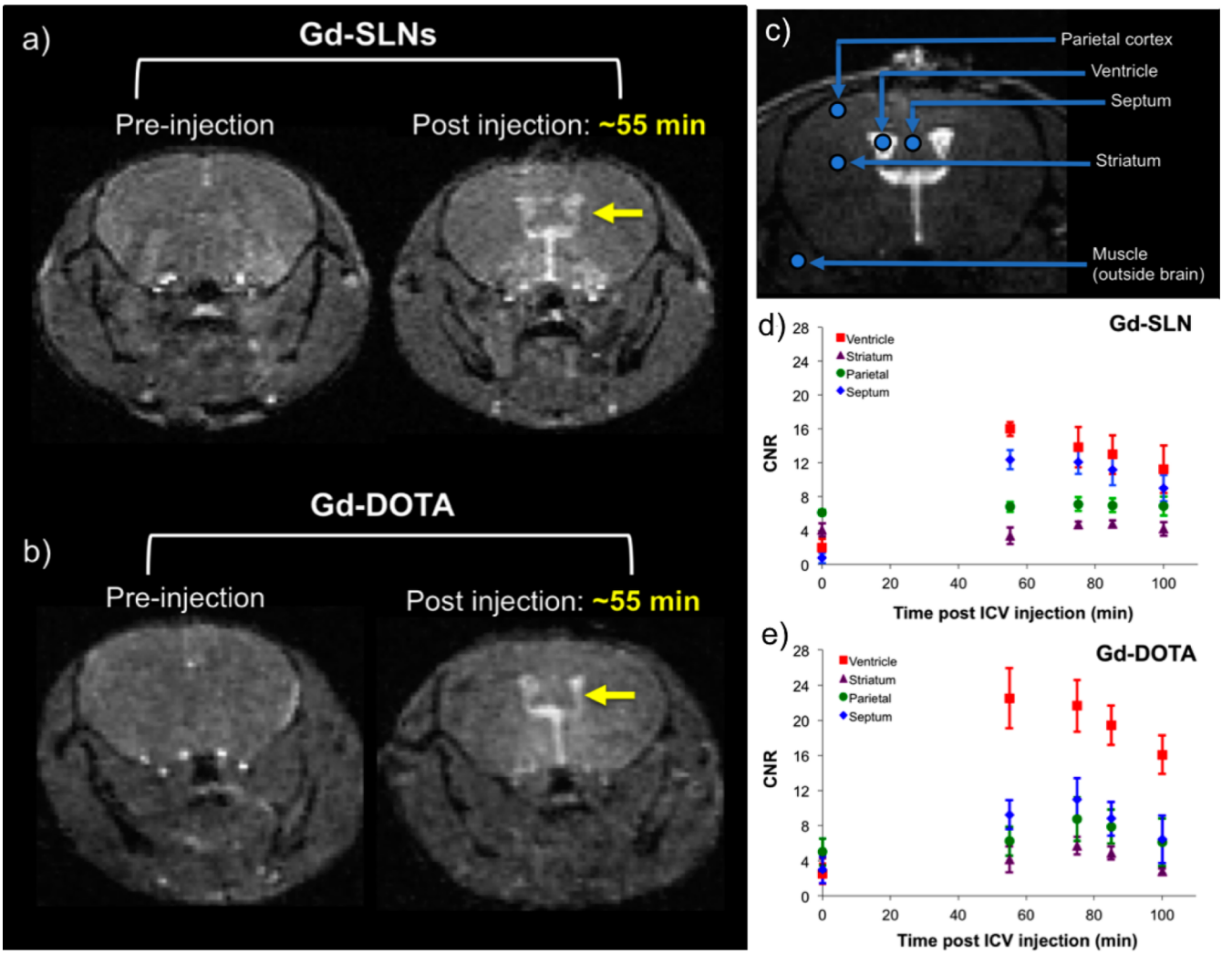

Figure 4. *In vivo* T_1w MRI of (a) Gd-SLNs (variation g, Table 1, ~150 nm) and (b) free Gd-DOTA following ICV injection in mice at 7T reveal similar positive contrast enhancement for both contrast agents (gradient echo image, TR/TE/α = 25 ms/2.75 ms/30°). Signal intensity was measured in representative regions of interest (ROI) displayed in (c) and used to calculate contrast-to-noise ratio (CNR) in the T_1w MR images. The CNR inside the ventricles increases drastically following ICV injection of the Gd-SLNs (d) and the free Gd-DOTA (e) but then decreases over time up to ~100 min. Aside from the ventricles and septum, the CNR inside the other brain regions (striatum and parietal cortex) changed minimally following ICV injection of Gd-SLNs (variation g, Table 1, ~150 nm) and free Gd-DOTA, remaining relatively constant up to ~100 min. Value = mean ± standard error of the mean, n = 3 animals per group.

and 4.5 mM) demonstrate that the positive contrast (bright signal) of the solution increases with increased Gd concentration (Figure 3a). We also recorded T_1w MR gradient echo images of tubes of nanopure water, Gd-SLNs (variation g, Table 1) and Gd-DOTA at the ICV concentration (1.525 mg Gd/mL, 9.7 mM) used *in vivo*. Gd-SLNs and Gd-DOTA showed a large signal enhancement as compared to nanopure water (Figure 3b). These data confirm that the Gd-SLNs can serve as an effective contrast agent for T_1w imaging at 7T by either spin echo or gradient echo acquisition protocols.

***T_1w* in Vivo MRI in Mice.** We then explored the signal changes that can be provided by Gd-SLNs *in vivo*. We focused on the brain ventricle as this is a well-characterized compartment for which we had prior data for free Gd-DOTA (unencapsulated) and in which Gd-DOTA is known to be detectable for at least two hours.[122,123] Studies in mice (n = 3 animals per group) after ICV injection of the Gd-SLNs (variation g, Table 1) or free Gd-DOTA (both at 1.525 mg Gd/mL, 9.7 mM) confirmed the ability of Gd-SLNs to provide positive contrast enhancement *in vivo* with T_1w MRI. As shown in Figure 4 from a representative animal, there was a similar increase in positive contrast from the preinjection to post-injection (~55 min) images of both Gd-SLNs (Figure 4a) and free Gd-DOTA (Figure 4b) at the site of the ventricles (yellow arrows).

Contrast to noise ratio (CNR) values were evaluated from theT_1w images in different regions of the brain (ventricle, septum, parietal cortex, and striatum; illustrated in Figure 4c) at various time points (~55, ~75, ~85, ~100 min; Figure 4d-e). The CNR inside the ventricles and septum evolved significantly with time for both the Gd-SLNs and the free Gd-DOTA (ANOVA, all ps <0.0001). Posthoc analyses confirmed a significant effect of time for each contrast agent taken individually (all ps <0.05). The CNR changes over time were very sharp from the 0 to 55 min time frames. Indeed, in the ventricle the CNR increased 726% and 802% for the Gd-SLNs (Figure 4d) and free Gd-DOTA (Figure 4e), respectively. In the septum, the signal increase was larger than 200% for both

dx.doi.org/10.1021/bc300605f | *Bioconjugate Chem.* XXXX, XXX, XXX–XXX

Gd-SLNs and free Gd-DOTA. In other brain regions (parietal cortex or striatum), the signal did not evolve with time (ANOVA, n.s) suggesting that the agents did not diffuse out of the ventricles and septum into these tissues. For all of the brain regions, the signal changes induced by Gd-SLNs were similar to those induced by Gd-DOTA (ANOVA, n.s.). This indicates that Gd-SLNs have the potential to be used as effective contrast agents for *in vivo* MRI.

Advantages of SLN-Encapsulated Contrast Agent and Potential Applications. Small Gd-based complexes such as Gd-DOTA are widely used as contrast agents for clinical MRI, and the incorporation of such complexes inside nanocarriers can offer improved pharmacokinetic properties, target specificity, multimodal functionality, and controlled release of the complexes for sustained T_1 contrast enhancement *in vivo* with MRI.[64] In general, the encapsulation of Gd-DOTA into SLNs has several advantages over the free cargo: (1) increased blood circulation time through protection from rapid kidney clearance; (2) multimodal functionality[117,124] by incorporation of an additional imaging moiety into the nanoparticle carrier; (3) targeted delivery through modifications at the particle surface;[65,82,125] (4) protection from degradation; and (5) the possibility of controlled Gd-DOTA release[14,82] for sustained T_1w positive contrast enhancement. Control over these properties is dependent upon SLN composition,[108] and future studies will involve thorough investigation of SLN degradation kinetics in order to effectively manipulate SLN composition for controlled release of Gd-DOTA.

SLNs offer many potential advantages over other drug carriers such as polymeric nanoparticles and liposomes for applications of MRI. Because SLNs are composed of naturally occurring physiological lipids, they exhibit high compatibility and biodegradability and have lower risk of toxicity than do polymeric nanoparticles.[2,3] Also, since SLNs are composed of a solid lipid core instead of the aqueous core characteristic of liposomes, they offer better protection against chemical degradation of their drug cargo than do liposomes.[2] Although liposomes have demonstrated successful encapsulation of paramagnetic payload ($MnCl_2$, Gd-DTPA, Mn-diethylenetriamine pentaacetic acid (Mn-DTPA), Gadodiamide (Gd-DTPA-MBA), Gadoteridol (Gd-HP-D03A)),[6,64] there is a tendency for the paramagnetic content inside their aqueous core to leak out of their permeable membranes, making the interpretation of observed contrast enhancement problematic.[64] This is less of an issue for SLNs because of the solid lipid core that acts as a membrane barrier to erosion and thus hinders encapsulated cargo from leaking outside the particle.

However, loading of hydrophilic cargo has been a major challenge in the field.[1,73,77,118,120,125−127] In the current article, we managed to create Gd-SLNs and focused on cerebral imaging to provide a proof of concept of the ability to induce signal changes in *in vivo* MR images with SLNs. We have demonstrated sufficient encapsulation of hydrophilic cargo (Gd-DOTA) into SLNs in order to generate adequate T_1w positive contrast enhancement that is similar to that of free Gd-DOTA. ICV injection enables one to observe contrast enhancement in a contained, localized region of the brain and thus was an effective model for evaluating *in vivo* contrast generated by the Gd-SLNs. We also showed that Gd-SLNs are able to cross the cerebral spinal fluid (CSF)-brain barrier since a signal increase was detected in the septum after administration of the Gd-SLN inside the ventricles.

In future studies, we will explore potential applications of Gd-SLNs. One such application is called gadolinium staining,[122] and it refers to the use of Gd-DOTA for detection of amyloid-beta (Aβ) plaques, the lesions of Alzheimer's disease (AD), by MRI in animal models. Gadolinium staining[122] has already demonstrated significant improvement in detecting Aβ plaques *in vivo* after intracerebroventricular (ICV) injection of Gd-DOTA into the brain parenchyma of transgenic AD mouse models[122] or intravenous injection of the contrast agent and opening of the blood brain barrier.[123] The ability to load Gd-DOTA into SLNs will allow tailoring of slow, controlled release of Gd-DOTA in the brain tissue in order to increase its lifetime or to optimize the targeting of SLNs to amyloid plaques.

Other applications include modifying SLNs with antibodies to target specific tissues. For example, Kuo et al. demonstrated the ability to target saquinavir (SQV)-loaded SLNs to human brain-microvascular endothelial cells (HBMECs) after modifying the SLN surface with the 83−14 monoclonal antibody (mAb). The receptor-mediated endocytosis of these 83−14 mAb-grafted SQV-loaded SLNs (83−14 mAb/SQV-SLNs) into human brain-microvascular endothelial cells (HBMECs) was confirmed with histology.[74]

Several studies also demonstrate the ability to modify SLNs for slow release. SLNs loaded with nisin, a natural antimicrobial agent, demonstrated antimicrobial activity up to 20 days in comparison to 3 days for free nisin.[97] Similarly, SLNs loaded with the antiviral agent, yak interferon-alpha (IFN-alpha), demonstrated both IFN-alpha release and antiviral activity up to 16 days.[128]

Even more, Gd-SLNs can be useful for imaging applications calling for longer residence of Gd-DOTA. Indeed, we have previously reported a longer blood half-life (~1.2 h) for SLNs[54] in comparison to Gd-DOTA (~3 min). Thus Gd-SLNs may be useful in angiography applications that require sustained MRI contrast in the vasculature over longer periods of time. This agrees with results from another groups demonstrating longer vasculature retention of Gd-lipid particles (Gd-LNPs) when compared to free Gd-DTPA; they attributed the Gd-LNPs' longer blood residence to their biliary versus renal clearance.[62]

An additional advantage of SLNs is that they have great potential as multimodal imaging agents because they can be radiolabeled using lipid chelator conjugates, as previously demonstrated by our group.[54] In this way, a radiolabel could be used to track the SLN carrier while MRI can be used to track the cargo.

CONCLUSION

In conclusion, we have synthesized monodisperse (hydrodynamic diameter = 151.0 ± 4.0 nm, polydispersity index = 0.25) SLNs loaded with Gd-DOTA for T_1w MRI. This demonstrates that hydrophilic metal complexes such as Gd-DOTA can be incorporated into SLNs. Through systematic variations to the W/O/W double microemulsion synthesis, we determined that optimizing the amount of low hydrophilic−lipophilic balance (HLB) surfactant, Span 80, to the "oil" phase significantly increased incorporation of hydrophilic cargo (Gd-DOTA) and resulted in a 25% increase of longitudinal relaxivity (r_1) leading to a relaxivity similar to that of free Gd-DOTA agents. The stability of particle size and stability of cargo encapsulation were verified over time. The significant enhancement of T_1 contrast for solution and *in vivo* MRI at 7T was observed after ICV injection of these Gd-SLNs into mice. SLN-encapsulated MRI contrast agents represent a new carrier to

protect diagnostic agents from degradation/clearance and holds the potential to extend to advantages of SLN to the delivery of these diagnostic agents.

AUTHOR INFORMATION

Corresponding Author

*Phone: 530-752-7134, e-mail: aylouie@ucdavis.edu.

Present Address

Erica Andreozzi, Kings College London, Division of Imaging Sciences and Biomedical Engineering, The Rayne Institute, 4th Floor Lambeth Wing, St. Thomas Hospital, London, UK SE1 7EH.

Notes

The authors declare no competing financial interest.

ACKNOWLEDGMENTS

We thank the France-Berkeley Fund and the National Institute of Health (EB000993, NS 40489, and NS060880) for their financial support of this work. We also thank the help of Joel Commisso at the Interdisciplinary Center for Plasma Mass Spectrometry at the University of California at Davis for assisting with the ICP-MS measurements. Lastly, we would like to thank Grete Adamson from the Electron Microscopy Laboratory (Department of Pathology and Laboratory Medicine and School of Medicine) at the University of California at Davis for her services and expertise with the TEM measurements.

REFERENCES

(1) Almeida, A. J., and Souto, E. (2007) Solid lipid nanoparticles as a drug delivery system for peptides and proteins. *Adv. Drug Delivery Rev. 59*, 478−490.

(2) Mehnert, W., and Mäder, K. (2001) Solid lipid nanoparticles: Production, characterization and applications. *Adv. Drug Delivery Rev. 47*, 165−196.

(3) Blasi, P., Giovagnoli, S., Schoubben, A., Ricci, M., and Rossi, C. (2007) Solid lipid nanoparticles for targeted brain drug delivery. *Adv. Drug Delivery Rev. 59*, 454−477.

(4) Rawat, M., Singh, D., and Saraf, S. (2008) Lipid carriers: A versatile delivery vehicle for proteins and peptides. *J. Pharm. Soc. Jpn. 128*, 269−280.

(5) Muller, R. H., Mehnert, W., Lucks, J. S., Schwarz, C., Zurmuhlen, A., Weyhers, H., Freitas, C., and Ruhl, D. (1995) Solid lipid nanoparticles (SLN)- An alternative colloidal carrier system for controlled drug-delivery. *Eur. J. Pharm. Biopharm. 41*, 62−69.

(6) Martins, S., Sarmento, B., Ferreira, D. C., and Souto, E. B. (2007) Lipid-based colloidal carriers for peptide and protein delivery - liposomes versus lipid nanoparticles. *Int. J. Nanomed. 2*, 595−607.

(7) zur Mühlen, A., Schwarz, C., and Mehnert, W. (1998) Solid lipid nanoparticles (SLN) for controlled drug delivery - Drug release and release mechanism. *Eur. J. Pharm. Biopharm. 45*, 149−155.

(8) Muller, R. H., Mader, K., and Gohla, S. (2000) Solid lipid nanoparticles (SLN) for controlled drug delivery - a review of the state of the art. *Eur. J. Pharm. Biopharm. 50*, 161−177.

(9) Baratchi, S., Kanwar, R. K., Khoshmanesh, K., Vasu, P., Ashok, C., Hittu, M., Parratt, A., Krishnakumar, S., Sun, X. Y., Sahoo, S. K., and Kanwar, J. R. (2009) Promises of nanotechnology for drug delivery to brain in neurodegenerative diseases. *Curr. Nanosci. 5*, 15−25.

(10) Rai, S., Paliwal, R., Gupta, P. N., Khatri, K., Goyal, A. K., Vaidya, B., and Vyas, S. P. (2008) Solid lipid nanoparticles (SLNs) as a rising tool in drug delivery science: One step up in nanotechnology. *Curr. Nanosci. 4*, 30−44.

(11) Uner, M. (2006) Preparation, characterization and physico-chemical properties of Solid Lipid Nanoparticles (SLN) and Nanostructured Lipid Carriers (NLC): Their benefits as colloidal drug carrier systems. *Pharmazie 61*, 375−386.

(12) Wang, S. P., Chen, T. K., Chen, R. E., Hu, Y. Y., Chen, M. W., and Wang, Y. T. (2012) Emodin loaded solid lipid nanoparticles: Preparation, characterization and antitumor activity studies. *Int. J. Pharm. 430*, 238−246.

(13) Olbrich, C., Kayser, O., and Muller, R. H. (2002) Lipase degradation of Dynasan 114 and 116 solid lipid nanoparticles (SLN) - effect of surfactants, storage time and crystallinity. *Int. J. Pharm. 237*, 119−128.

(14) Celia, C., Cosco, D., Paolino, D., and Fresta, M. (2011) Nanoparticulate devices for brain drug delivery. *Med. Res. Rev. 31*, 716−756.

(15) Kaur, I. P., Bhandari, R., Bhandari, S., and Kakkar, V. (2008) Potential of solid lipid nanoparticles in brain targeting. *J. Controlled Release 127*, 97−109.

(16) Gupta, Y., Jain, A., and Jain, S. K. (2007) Transferrin-conjugated solid lipid nanoparticles for enhanced delivery of quinine dihydrochloride to the brain. *J. Pharm. Pharmacol. 59*, 935−940.

(17) Jain, S. K., Chaurasiya, A., Gupta, Y., Jain, A., Dagur, P., Joshi, B., and Katoch, V. M. (2008) Development and characterization of 5-FU bearing ferritin appended solid lipid nanoparticles for tumour targeting. *J. Microencapsulation 25*, 289−297.

(18) Reddy, L., Sharma, R., Chuttani, K., Mishra, A., and Murthy, R. (2005) Influence of administration route on tumro uptake and biodistribution of etoposide loaded solid lipid nanoparticles in Dalton's Lymphoma tumor bearing mice. *J. Controlled Release 105*, 185−198.

(19) Yassin, A. E. B., Anwer, M. K., Mowafy, H. A., El-Bagory, I. M., Bayomi, M. A., and Alsarra, I. A. (2010) Optimization of 5-fluorouracil solid-lipid nanoparticles: a preliminary study to treat colon cancer. *Int. J. Med. Sci. 7*, 398−408.

(20) Lu, B., Xiong, S. B., Yang, H., Yin, X. D., and Chao, R. B. (2006) Solid lipid nanoparticles of mitoxantrone for local injection against breast cancer and its lymph node metastases. *Eur. J. Pharm. Sci. 28*, 86−95.

(21) Seyfoddin, A., Shaw, J., and Al-Kassas, R. (2010) Solid lipid nanoparticles for ocular drug delivery. *Drug Delivery 17*, 467−489.

(22) Li, R., Jiang, S. M., Liu, D. F., Bi, X. Y., Wang, F. Z., Zhang, Q., and Xu, Q. W. (2011) A potential new therapeutic system for glaucoma: solid lipid nanoparticles containing methazolamide. *J. Microencapsulation 28*, 134−141.

(23) Kalam, M. A., Sultana, Y., Ali, A., Aqil, M., Mishra, A. K., and Chuttani, K. (2010) Preparation, characterization, and evaluation of gatifloxacin loaded solid lipid nanoparticles as colloidal ocular drug delivery system. *J. Drug Target 18*, 191−204.

(24) Gokce, E. H., Sandri, G., Bonferoni, M. C., Rossi, S., Ferrari, F., Guneri, T., and Caramella, C. (2008) Cyclosporine A loaded SLNs: Evaluation of cellular uptake and corneal cytotoxicity. *Int. J. Pharm. 364*, 76−86.

(25) Jaafar-Maalej, C., Andrieu, V., Elaissari, A., and Fessi, H. (2011) Beclomethasone-loaded lipidic nanocarriers for pulmonary drug delivery: preparation, characterization and in vitro drug release. *J. Nanosci. Nanotechnol. 11*, 1841−1851.

(26) Sanna, V., Kirschvink, N., Gustin, P., Gavini, E., Roland, I., Delattre, L., and Evrard, B. (2004) Preparation and in vivo toxicity study of solid lipid microparticles as carrier for pulmonary administration. *AAPS PharmSciTech 5*.

(27) Nassimi, M., Schleh, C., Lauenstein, H. D., Hussein, R., Hoymann, H. G., Koch, W., Pohlmann, G., Krug, N., Sewald, K., Rittinghausen, S., Braun, A., and Muller-Goymann, C. (2010) A toxicological evaluation of inhaled solid lipid nanoparticles used as a potential drug delivery system for the lung. *Eur. J. Pharm. Biopharm. 75*, 107−116.

(28) Souto, E. B., Wissing, S. A., Barbosa, C. M., and Muller, R. H. (2004) Development of a controlled release formulation based on SLN and NLC for topical clotrimazole delivery. *Int. J. Pharm. 278*, 71−77.

(29) Jain, S. K., Chourasia, M. K., Masuriha, R., Soni, V., Jain, A., Jain, N. K., and Gupta, Y. (2005) Solid lipid nanoparticles bearing flurbiprofen for transdermal delivery. *Drug Delivery 12*, 207−215.
(30) Mandawgade, S. D., and Patravale, V. B. (2008) Development of SLNs from natural lipids: Application to topical delivery of tretinoin. *Int. J. Pharm. 363*, 132−138.
(31) Maia, C. S., Mehnert, W., and Schafer-Korting, M. (2000) Solid lipid nanoparticles as drug carriers for topical glucocorticoids. *Int. J. Pharm. 196*, 165−167.
(32) Uner, M., and Yener, G. (2007) Importance of solid lipid nanoparticles (SLN) in various administration routes and future perspectives. *Int. J. Nanomed. 2*, 289−300.
(33) Wissing, S. A., and Muller, R. H. (2002) Solid lipid nanoparticles as carrier for sunscreens: in vitro release and in vivo skin penetration. *J. Controlled Release 81*, 225−233.
(34) Maia, C. S., Mehnert, W., Schaller, M., Korting, H. C., Gysler, A., Haberland, A., and Schafer-Korting, M. (2002) Drug targeting by solid lipid nanoparticles for dermal use. *J. Drug Targeting 10*, 489−495.
(35) Vighi, E., and Leo, E. (2012) Studying the in vitro behavior of cationic solid lipid nanoparticles as a nonviral vector. *Nanomedicine 7*, 9−12.
(36) Vighi, E., Montanari, M., Ruozi, B., Iannuccelli, V., and Leo, E. (2012) The role of protamine amount in the transfection performance of cationic SLN designed as a gene nanocarrier. *Drug Delivery 19*, 1−10.
(37) Jin, J., Bae, K. H., Yang, H., Lee, S. J., Kim, H., Kim, Y., Joo, K. M., Seo, S. W., Park, T. G., and Nam, D. H. (2011) In vivo specific delivery of c-Met siRNA to glioblastoma using cationic solid lipid nanoparticles. *Bioconjugate Chem. 22*, 2568−2572.
(38) Wen, C. J., Yen, T. C., Al-Suwayeh, S. A., Chang, H. W., and Fang, J. Y. (2011) In vivo real-time fluorescence visualization and brain-targeting mechanisms of lipid nanocarriers with different fatty ester:oil ratios. *Nanomedicine 6*, 1545−1559.
(39) Ye, J. S., Wang, A. H., Liu, C. X., Chen, Z. J., and Zhang, N. (2008) Anionic solid lipid nanoparticles supported on protamine/DNA complexes. *Nanotechnology 19*, 285708−285717.
(40) Kuo, Y. C., and Wang, C. C. (2010) Electrophoresis of human brain microvascular endothelial cells with uptake of cationic solid lipid nanoparticles: Effect of surfactant composition. *Colloids Surf., B: Biointerfaces 76*, 286−291.
(41) Vighi, E., Montanari, M., Ruozi, B., Tosi, G., Magli, A., and Leo, E. (2010) Nuclear localization of cationic solid lipid nanoparticles containing Protamine as transfection promoter. *Eur. J. Pharm. Biopharm. 76*, 384−393.
(42) Agarwal, A., Majumder, S., Agrawal, H., Majumdar, S., and Agrawal, G. P. (2011) Cationized albumin conjugated solid lipid nanoparticles as vectors for brain delivery of an anti-cancer drug. *Curr. Nanosci. 7*, 71−80.
(43) Doroud, D., Vatanara, A., Zahedifard, F., Gholami, E., Vahabpour, R., Najafabadi, A. R., and Rafati, S. (2010) Cationic solid lipid nanoparticles loaded by cysteine proteinase genes as a novel anti-leishmaniasis DNA vaccine delivery system: characterization and in vitro evaluations. *J. Pharm. Pharm. Sci. 13*, 320−335.
(44) Taveira, S. F., Araujo, L., de Santana, D., Nomizo, A., de Freitas, L. A. P., and Lopez, R. F. V. (2012) Development of cationic solid lipid nanoparticles with factorial design-based studies for topical administration of doxorubicin. *J. Biomed. Nanotechnol. 8*, 219−228.
(45) Choi, S. H., Jin, S. E., Lee, M. K., Lim, S. J., Park, J. S., Kim, B. G., Ahn, W. S., and Kim, C. K. (2008) Novel cationic solid lipid nanoparticles enhanced p53 gene transfer to lung cancer cells. *Eur. J. Pharm. Biopharm 68*, 545−554.
(46) Goppert, T. M., and Muller, R. H. (2005) Polysorbate-stabilized solid lipid nanoparticles as colloidal carriers for intravenous targeting of drugs to the brain: Comparison of plasma protein adsorption patterns. *J. Drug Target 13*, 179−187.
(47) Sanjula, B., Shah, F. M., Javed, A., and Alka, A. (2009) Effect of poloxamer 188 on lymphatic uptake of carvedilol-loaded solid lipid nanoparticles for bioavailability enhancement. *J. Drug Target 17*, 249−256.
(48) Kreuter, J., Shamenkov, D., Petrov, V., Ramge, P., Cychutek, K., Koch-Brandt, C., and Alyautdin, R. (2002) Apolipoprotein-mediated transport of nanoparticle-bound drugs across the blood-brain barrier. *J. Drug Target 10*, 317−325.
(49) Koffie, R. M., Farrar, C. T., Saidi, L. J., William, C. M., Hyman, B. T., and Spires-Jones, T. L. (2011) Nanoparticles enhance brain delivery of blood-brain barrier-impermeable probes for in vivo optical and magnetic resonance imaging. *Proc. Natl. Acad. Sci. U. S. A. 108*, 18837−18842.
(50) Tian, X. H., Lin, X. N., Wei, F., Feng, W., Huang, Z. C., Wang, P., Ren, L., and Diao, Y. (2011) Enhanced brain targeting of Temozolomide in polysorbate-80 coated polybutylcyanoacrylate nanoparticles. *Int. J. Nanomed. 6*, 445−452.
(51) Sarmento, B., Mazzaglia, D., Bonferoni, M. C., Neto, A. P., Monteiro, M. D., and Seabra, V. (2011) Effect of chitosan coating in overcoming the phagocytosis of insulin loaded solid lipid nanoparticles by mononuclear phagocyte system. *Carbohydr. Polym. 84*, 919−925.
(52) Malhotra, M., and Prakash, S. (2011) Targeted drug delivery across blood-brain-barrier using cell penetrating peptides tagged nanoparticles. *Curr. Nanosci. 7*, 81−93.
(53) Stevens, P. J., Sekido, M., and Lee, R. J. (2004) Synthesis and evaluation of a hematoporphyrin derivative in a folate receptor-targeted solid-lipid nanoparticle formulation. *Anticancer Res. 24*, 161−165.
(54) Andreozzi, E., Seo, J. W., Ferrara, K., and Louie, A. (2011) Novel method to label solid lipid nanoparticles with (64)Cu for positron emission tomography imaging. *Bioconjugate Chem. 22*, 808−818.
(55) Videira, M. A., Gano, L., Santos, C., Neves, M., and Almeida, A. J. (2006) Lymphatic uptake of lipid nanoparticles following endotracheal administration. *J. Microencapsulation 23*, 855−862.
(56) Liu, W., Liang, J. G., Zhu, Y. L., Xu, H. B., He, Z. K., and Yang, X. L. (2006) CdSe/ZnS quantum dots loaded solid lipid nanoparticles: Novel luminescent nanocomposite particles, in *Eco-Materials Processing & Design Vii* (Kim, H. S., Li, Y. B., and Lee, S. W., Eds.) pp 170−173, Trans Tech Publications Ltd, Zurich-Uetikon.
(57) Reimold, I., Domke, D., Bender, B., Seyfried, C., Radunz, H., and Fricker, G. (2008) Delivery of nanoparticles to the brain detected by fluorescence microscopy. *Eur. J. Pharm. Biopharm. 70*, 627−632.
(58) Liu, W., He, Z. K., Liang, J. G., Zhu, Y. L., Xu, H. B., and Yang, X. L. (2008) Preparation and characterization of novel fluorescent nanocomposite particles: CdSe/ZnS core-shell quantum dots loaded solid lipid nanoparticles. *J. Biomed. Mater. Res., Part A 84A*, 1018−1025.
(59) Chen, D. B., Yang, T. Z., Lu, W. L., and Zhang, Q. (2001) In vitro and in vivo study of two types of long-circulating solid lipid nanoparticles containing paclitaxel. *Chem. Pharm. Bull. 49*, 1444−1447.
(60) Esposito, E., Fantin, M., Marti, M., Drechsler, M., Paccamiccio, L., Mariani, P., Sivieri, E., Lain, F., Menegatti, E., Morari, M., and Cortesi, R. (2008) Solid lipid nanoparticles as delivery systems for bromocriptine. *Pharm. Res. 25*, 1521−1530.
(61) Fundaro, A., Cavalli, R., Bargoni, A., Vighetto, D., Zara, G. P., and Gasco, M. R. (2000) Non-stealth and stealth solid lipid nanoparticles (SLN) carrying doxorubicin: Pharmacokinetics and tissue distribution after i.v. administration to rats. *Pharmacol. Res. 42*, 337−343.
(62) Bui, T., Stevenson, J., Hoekman, J., Zhang, S. R., Maravilla, K., and Ho, R. J. Y. (2010) Novel Gd nanoparticles enhance vascular contrast for high-resolution magnetic resonance imaging. *Plos One 5*, e13082.
(63) Peira, E., Marzola, P., Podio, V., Aime, S., Sbarbati, A., and Gasco, M. R. (2003) In vitro and in vivo study of solid lipid nanoparticles loaded with superparamagnetic iron oxide. *J. Drug Target 11*, 19−24.
(64) Mulder, W. J. M., Strijkers, G. J., van Tilborg, G. A. F., Griffioen, A. W., and Nicolay, K. (2006) Lipid-based nanoparticles for contrast-enhanced MRI and molecular imaging. *NMR Biomed. 19*, 142−164.

(65) Beduneau, A., Hindre, F., Clavreul, A., Leroux, J. C., Saulnier, P., and Benoit, J. P. (2008) Brain targeting using novel lipid nanovectors. *J. Controlled Release 126*, 44−49.
(66) Sun, J. H., Zheng, W. L., Zhang, H., Wu, T., Yuan, H., Yang, X. M., and Zhang, S. Z. (2011) Development of nanoparticle-based magnetic resonance colonography. *Magn. Reson. Med. 65*, 673−679.
(67) Hu, F. Q., Hong, Y., and Yuan, H. (2004) Preparation and characterization of solid lipid nanoparticles containing peptide. *Int. J. Pharm. 273*, 29−35.
(68) Zhang, Z. H., Lv, H. X., and Zhou, J. P. (2009) Novel solid lipid nanoparticles as carriers for oral administration of insulin. *Pharmazie 64*, 574−578.
(69) Jiao, J., and Burgess, D. J. (2003) Rheology and stability of water-in-oil-in-water multiple emulsions containing Span 83 and Tween 80. *AAPS PharmSci 5*, 62−73.
(70) Ugazio, E., Cavalli, R., and Gasco, M. R. (2002) Incorporation of cyclosporin A in solid lipid nanoparticles (SLN). *Int. J. Pharm. 241*, 341−344.
(71) Li, Z., Li, X. W., Zheng, L. Q., Lin, X. H., Geng, F., and Yu, L. (2010) Bovine serum albumin loaded solid lipid nanoparticles prepared by double emulsion method. *Chem. Res. Chin. Univ. 26*, 136−141.
(72) Xie, S. Y., Wang, S. L., Zhao, B. K., Han, C., Wang, M., and Zhou, W. Z. (2008) Effect of PLGA as a polymeric emulsifier on preparation of hydrophilic protein-loaded solid lipid nanoparticles. *Colloids Surf., B: Biointerfaces 67*, 199−204.
(73) Gallarate, M., Trotta, M., Battaglia, L., and Chirio, D. (2009) Preparation of solid lipid nanoparticles from W/O/W emulsions: Preliminary studies on insulin encapsulation. *J. Microencapsulation 26*, 394−402.
(74) Ce, Q., Yan, C., Qing-Zhe, J., and Xing-Guo, W. (2011) Preparation and characterization of catalase-loaded solid lipid nanoparticles protecting enzyme against proteolysis. *J. Mol. Sci. 12*, 4282−4293.
(75) Chambi, H. N. M., Alvim, I. D., Barrera-Arellano, D., and Grosso, C. R. F. (2008) Solid lipid microparticles containing water-soluble compounds of different molecular mass: Production, characterisation and release profiles. *Food Res. Int. 41*, 229−236.
(76) Garcia-Fuentes, M., Torres, D., and Alonso, M. J. (2003) Design of lipid nanoparticles for the oral delivery of hydrophilic macromolecules. *Colloids Surf., B: Biointerfaces 27*, 159−168.
(77) Singh, S., Dobhal, A. K., Jain, A., Pandit, J. K., and Chakraborty, S. (2010) Formulation and evaluation of solid lipid nanoparticles of a water soluble drug: zidovudine. *Chem. Pharm. Bull. 58*, 650−655.
(78) You, J., Wan, F., de Cui, F., Sun, Y., Du, Y.-Z., and Hu, F. Q. (2007) Preparation and characteristic of vinorelbine bitartrate-loaded solid lipid nanoparticles. *Int. J. Pharm. 343*, 270−276.
(79) Liu, J., Gong, T., Wang, C. G., Zhong, Z. R., and Zhang, Z. R. (2007) Solid lipid nanoparticles loaded with insulin by sodium cholate-phosphatidylcholine-based mixed micelles: Preparation and characterization. *Int. J. Pharm. 340*, 153−162.
(80) O'Brien, J., Wilson, I., Orton, T., and Pognan, F. (2000) Investigation of the Alamar Blue (resazurin) fluorescent dye for the assessment of mammalian cell cytotoxicity. *Eur. J. Biochem. 267*, 5421−5426.
(81) Paxinos, G., and Franklin, K. (2001) *The Mouse Brain in Stereotaxic Coordinates*, 2nd ed., pp 107−120, Academic Press, San Diego.
(82) Mukherjee, S., Ray, S., and Thakur, R. S. (2009) Solid lipid nanoparticles: a modern formulation approach in drug delivery system. *Indian Journal of Pharmaceutical Sciences 71*, 349−358.
(83) Saha, R. N., Vasanthakumar, S., Bende, G., and Snehalatha, M. (2010) Nanoparticulate drug delivery systems for cancer chemotherapy. *Mol. Membr. Biol. 27*, 215−231.
(84) Moghimi, S. M., Hunter, A. C., and Murray, J. C. (2001) Long-circulating and target-specific nanoparticles: Theory to practice. *Pharmacol. Rev. 53*, 283−318.
(85) Barbu, E., Molnar, E., Tsibouklis, J., and Gorecki, D. C. (2009) The potential for nanoparticle-based drug delivery to the brain: overcoming the blood-brain barrier. *Expert Opin. Drug Delivery 6*, 553−565.
(86) Mohapatra, M., and Mishra, A. K. (2011) Effect of submicellar concentrations of conjugated and unconjugated bile salts on the lipid bilayer membrane. *Langmuir 27*, 13461−13467.
(87) Albalak, A., Zeidel, M. L., Zucker, S. D., Jackson, A. A., and Donovan, J. M. (1996) Effects of submicellar bile salt concentrations on biological membrane permeability to low molecular weight non-ionic solutes. *Biochemistry 35*, 7936−7945.
(88) Rotunda, A. M., Suzuki, H., Moy, R. L., and Kolodney, M. S. (2004) Detergent effects of sodium deoxycholate are a major feature of an injectable phosphatidylcholine formulation used for localized fat dissolution. *Dermatol. Surg. 30*, 1001−1008.
(89) Cardenas, M., Schillen, K., Alfredsson, V., Duan, R. D., Nyberg, L., and Amebrant, T. (2008) Solubilization of sphingornyelin vesicles by addition of a bile salt. *Chem. Phys. Lipids 151*, 10−17.
(90) Suzuki, K., Hasegawa, T., Takamura, Y., Takahashi, K., Asano, H., and Ueno, M. (1996) Behaviors of sodium taurocholate and sodium taurodeoxycholate in binary mixed micelles of bile salt and nonionic surfactant. *Langmuir 12*, 5536−5540.
(91) Sjostrom, B., Kaplun, A., Talmon, Y., and Cabane, B. (1995) Structures of nanoparticles prepared from oil-in-water emulsions. *Pharm. Res. 12*, 39−48.
(92) Triplett, M. D., and Rathman, J. F. (2009) Optimization of beta-carotene loaded solid lipid nanoparticles preparation using a high shear homogenization technique. *J. Nanopart. Res. 11*, 601−614.
(93) Siekmann, B., and Westesen, K. (1996) Investigations on solid lipid nanoparticles prepared by precipitation in o/w emulsions. *Eur. J. Pharm. Biopharm. 42*, 104−109.
(94) Rupp, C., Steckel, H., and Muller, B. W. (2010) Mixed micelle formation with phosphatidylcholines: The influence of surfactants with different molecule structures. *Int. J. Pharm. 387*, 120−128.
(95) You, J., Wan, F., de Cui, F., Sun, Y., Du, Y. Z., and Hu, F. Q. (2007) Preparation and characteristic of vinorelbine bitartrate-loaded solid lipid nanoparticles. *Int. J. Pharm. 343*, 270−276.
(96) Kovacevic, A., Savic, S., Vuleta, G., Muller, R. H., and Keck, C. M. (2011) Polyhydroxy surfactants for the formulation of lipid nanoparticles (SLN and NLC): Effects on size, physical stability and particle matrix structure. *Int. J. Pharm. 406*, 163−172.
(97) Prombutara, P., Kulwatthanasal, Y., Supaka, N., Sramala, I., and Chareonpornwattana, S. (2012) Production of nisin-loaded solid lipid nanoparticles for sustained antimicrobial activity. *Food Control 24*, 184−190.
(98) Accardo, A., Tesauro, D., Aloj, L., Pedone, C., and Morelli, G. (2009) Supramolecular aggregates containing lipophilic Gd(III) complexes as contrast agents in MRI. *Coord. Chem. Rev. 253*, 2193−2213.
(99) Villaraza, A. J. L., Bumb, A., and Brechbiel, M. W. (2010) Macromolecules, dendrimers, and nanomaterials in magnetic resonance imaging: the interplay between size, function, and pharmacokinetics. *Chem. Rev. 110*, 2921−2959.
(100) Yuan, H., Jiang, S. P., Du, Y. Z., Miao, J., Zhang, X. G., and Hu, F. Q. (2009) Strategic approaches for improving entrapment of hydrophilic peptide drugs by lipid nanoparticles. *Colloids Surf., B: Biointerfaces 70*, 248−253.
(101) Villa, C. H., Lawson, L. B., Li, Y. M., and Papadopoulos, K. D. (2003) Internal coalescence as a mechanism of instability in water-in-oil-in-water double-emulsion globules. *Langmuir 19*, 244−249.
(102) Caravan, P., Ellison, J. J., McMurry, T. J., and Lauffer, R. B. (1999) Gadolinium(III) chelates as MRI contrast agents: Structure, dynamics, and applications. *Chem. Rev. 99*, 2293−2352.
(103) Tu, C. Q., Osborne, E. A., and Louie, A. Y. (2011) Activatable T (1) and T (2) magnetic resonance imaging contrast agents. *Ann. Biomed. Eng. 39*, 1335−1348.
(104) Olbrich, C., and Muller, R. H. (1999) Enzymatic degradation of SLN - effect of surfactant and surfactant mixtures. *Int. J. Pharm. 180*, 31−39.
(105) Silva, A. C., Gonzalez-Mira, E., Garcia, M. L., Egea, M. A., Fonseca, J., Silva, R., Santos, D., Souto, E. B., and Ferreira, D. (2011)

Preparation, characterization and biocompatibility studies on risperidone-loaded solid lipid nanoparticles (SLN): High pressure homogenization versus ultrasound. *Colloids Surf., B: Biointerfaces 86*, 158−165.
(106) Scholer, N., Zimmermann, E., Katzfey, U., Hahn, H., Muller, R. H., and Liesenfeld, O. (2000) Preserved solid lipid nanoparticles (SLN) at low concentrations do cause neither direct nor indirect cytotoxic effects in peritoneal macrophages. *Int. J. Pharm. 196*, 235−239.
(107) Martins, S., Costa-Lima, S., Carneiro, T., Cordeiro-da-Silva, A., Souto, E. B., and Ferreira, D. C. (2012) Solid lipid nanoparticles as intracellular drug transporters: An investigation of the uptake mechanism and pathway. *Int. J. Pharm. 430*, 216−227.
(108) Weyhers, H., Ehlers, S., Hahn, H., Sout, E. B., and Muller, R. H. (2006) Solid lipid nanoparticles (SLN) - Effects of lipid composition on in vitro degradation and in vivo toxicity. *Pharmazie 61*, 539−544.
(109) Schöler, N., Olbrich, C., Tabatt, K., Müller, R. H., Hahn, H., and Liesenfeld, O. (2001) Surfactant, but not the size of solid lipid nanoparticles (SLN) influences viability and cytokine production of macrophages. *Int. J. Pharm. 221*, 57−67.
(110) Olbrich, C., Scholer, N., Tabatt, K., Kayser, O., and Muller, R. H. (2004) Cytotoxicity studies of Dynasan 114 solid lipid nanoparticles (SLN) on RAW 264.7 macrophages - impact of phagocytosis on viability and cytokine production. *J. Pharm. Pharmacol. 56*, 883−891.
(111) Müller, R. H., Maassen, S., Schwarz, C., and Mehnert, W. (1997) Solid lipid nanoparticles (SLN) as potential carrier for human use: interaction with human granulocytes. *J. Controlled Release 47*, 261−269.
(112) Cavalli, R., Bocca, C., Miglietta, A., Caputo, O., and Gasco, M. R. (1999) Albumin adsorption on stealth and non-stealth solid lipid nanoparticles. *STP Pharma Sci. 9*, 183−189.
(113) Bocca, C., Caputo, O., Cavalli, R. B., Gabriel, L., Miglietta, A., and Gasco, M. R. (1998) Phagocytic uptake of fluorescent stealth and non-stealth solid lipid nanoparticles. *Int. J. Pharm. 175*, 185−193.
(114) Illum, L., Davis, S. S., Muller, R. H., Mak, E., and West, P. (1987) The organ biodistribution and circulation time of intravenously injected colloidal carriers sterically stabilized with a blockcopolymer-poloxamine 908. *Life Sci. 40*, 367−374.
(115) Muller, R. H., Maassen, S., Weyhers, H., and Mehnert, W. (1996) Phagocytic uptake and cytotoxicity of solid lipid nanoparticles (SLN) sterically stabilized with poloxamine 908 and poloxamer 407. *J. Drug Target 4*, 161−170.
(116) Muller, R. H., Maassen, S., Weyhers, H., Specht, F., and Lucks, J. S. (1996) Cytotoxicity of magnetite-loaded polylactide, polylactide/glycolide particles and solid lipid nanoparticles. *Int. J. Pharm. 138*, 85−94.
(117) Mehnert, W., and Mader, K. (2012) Solid lipid nanoparticles Production, characterization and applications. *Adv. Drug Delivery Rev. 64*, 83−101.
(118) Liu, H., Gong, T., Fu, H. L., Wang, C. G., Wang, X. L., Chen, Q., Zhang, Q., He, Q., and Zhang, Z. R. (2008) Solid lipid nanoparticles for pulmonary delivery of insulin. *Int. J. Pharm. 356*, 333−344.
(119) Zhou, H. F., Ma, Q. H., Xia, Q., Lu, Y. Y., Gu, N., Miao, X., and Luo, D. (2007) Preparation and cytotoxicity of imiquimod-loaded solid lipid nanoparticles, in *Nanoscience and Technology, Pts 1 and 2* (Bai, C., Xie, S., and Zhu, X., Eds.) pp 271−274, Trans Tech Publications Ltd, Stafa-Zurich.
(120) Joshi, M. D., and Müller, R. H. (2009) Lipid nanoparticles for parenteral delivery of actives. *Eur. J. Pharm. Biopharm. 71*, 161−172.
(121) Nassimi, M., Schleh, C., Lauenstein, H.-D., Hussein, R., Lubbers, K., Pohlmann, G., Switalla, S., Sewald, K., Muller, M., Krug, N., Muller-Goymann, C. C., and Braun, A. (2009) Low cytotoxicity of solid lipid nanoparticles in in vitro and ex vivo lung models. *Inhalation Toxicol. 21* (Suppl 1), 104−9.
(122) Petiet, A., and Dhenain, M. (2011) Improvement of microscopic MR imaging of amyloid plaques with targeting and non-targeting contrast agents. *Curr. Med. Imaging Rev. 7*, 8−15.
(123) Blower, P. J., Lewis, J. S., and Zweit, J. (1996) Copper radionuclides and radiopharmaceuticals in nuclear medicine. *Nucl. Med. Biol. 23*, 957−980.
(124) Mulder, W. J. M., Strijkers, G. J., Van Tilborg, G. A. F., Cormode, D. P., Fayad, Z. A., and Nicolay, K. (2009) Nanoparticulate assemblies of amphiphiles and diagnostically active materials for multimodality imaging. *Acc. Chem. Res. 42*, 904−914.
(125) Harms, M., and Muller-Goymann, C. C. (2011) Solid lipid nanoparticles for drug delivery. *J. Drug Delivery Sci. Technol. 21*, 89−99.
(126) Morel, S., Ugazio, E., Cavalli, R., and Gasco, M. R. (1996) Thymopentin in solid lipid nanoparticles. *Int. J. Pharm. 132*, 259−261.
(127) Olbrich, C., Gessner, A., Schroder, W., Kayser, O., and Muller, R. H. (2004) Lipid-drug conjugate nanoparticles of the hydrophilic drug diminazene - cytotoxicity testing and mouse serum adsorption. *J. Controlled Release 96*, 425−435.
(128) Li, S. Y., Zhao, B. K., Wang, F. H., Wang, M., Xie, S. Y., Wang, S. L., Han, C., Zhu, L. Y., and Zhou, W. Z. (2010) Yak interferon-alpha loaded solid lipid nanoparticles for controlled release. *Res. Vet. Sci. 88*, 148−153.